Mineral. Soc. Amer. Spec. Pap. **2**, 101–109 (1969).

CRYSTAL STRUCTURE OF PROTOAMPHIBOLE

G. V. GIBBS

Department of Geological Sciences, Virginia Polytechnic Institute
Blacksburg, Virginia 24061

ABSTRACT

The structure proposed for protoamphibole (Gibbs *et al.*, 1960) has been verified and refined by three-dimensional Fourier and least-squares methods using data collected with a Weissenberg single crystal counter-diffractometer. The symmetry is *Pnmn* with $a = 9.330$, $b = 17.879$ and $c = 5.288$ Å and the unit-cell content is $2(Na_{0.03}Li_{1.20}Mg_{6.44})(Si_{7.84}Al_{0.04}O_{21.71})(OH_{0.15}F_{2.14})$.

The structure consists of layers of interlocking chains of fluorine-centered hexagonal rings of SiO_4 groups. The layers are bound together by Mg,Li cations which are coordinated between the chains, the coordination being effected by a $\sim(c/3)$ stagger between adjacent layers. An additional stagger of $\sim(-c/3)$ in the sequence along a gives an overall displacement of zero between alternate layers, accounting for the 9.33 Å a cell edge and the orthogonal geometry. The direction of stagger can be related to the placement of the cations in the octahedral layer. The M-cation coordination groups are nearly regular octahedra with the exception of $M(4)$ which is similar to Mg(1) in protoenstatite. The $M(3)$, $M(1)$ and $M(2)$ sites are occupied principally by Mg. In addition to being randomly distributed around the cavity walls of the A-site, Li ions are also segregated in about 25% of the $M(4)$ sites, the others being occupied by Mg ions. The individual Si-O bond distances in the chains are consistent with Cruickshank's d-p π bonding model: Si-O(non-bridging) bonds [Si(1)-O(1) = 1.592; Si(2)-O(4) = 1.592; Si(2)-O(2) = 1.605 Å] are significantly shorter, on the average, than the Si-O(bridging) bonds [Si(1)-O(5) = 1.616; Si(1)-O(6) = 1.623; Si(1)-O(7) = 1.624; Si(2)-O(5) = 1.626; Si(2)-O(6) = 1.655 Å]. The shortest O-O distance (2.495 Å) is an edge shared between the Si(2) and the $M(4)$ polyhedra.

INTRODUCTION

As part of a detailed study to establish the crystal chemistry of the amphibole and pyroxene minerals, Warren and Bragg (1928) undertook a structural analysis of the clinopyroxene, diopside, $CaMgSi_2O_6$. Its cell edges and space-group symmetry (Table 1) were determined by rotating crystal techniques and its structure was deduced by a clever trial and error method. The basic unit in the diopside structure was found to be a single chain of $(SiO_3)_\infty$ composition. The structure of clinoamphibole was established two years later by Warren (1929) who undertook a similar study of tremolite, $Ca_2Mg_5(Si_4O_{11})_2(OH_2)$, and found the tremolite rotation photographs to be remarkably similar to those of diopside. The cell edges, a and c, and the β angle (Table 1) were found to be practically identical and b just double that measured for diopside; furthermore, the positions and intensities of the $h0l$ reflections were in close agreement, spot for spot. This indicated that when viewed down b diopside and tremolite are nearly indistinguishable. However, tremolite ($C2/m$) does differ from diopside in that its space group contains mirror planes parallel to (010) whereas diopside ($C2/c$) contains c-glide planes instead. This information led Warren to introduce a "block" of the diopside structure directly into the unit cell of tremolite in such a way that the mirror parallel to (010) doubled the single chains to double chains of $(Si_4O_{11})_\infty$ composition and accordingly, the b axis. The structure of tremolite was then generated from the "block" by the rotational and translational symmetry operators of $C2/m$, following a centering of the hexagonal ring by a hydroxyl group and a placing of a magnesium cation at the origin. In a later paper (Warren and Modell, 1930), the structure of the orthorhombic amphibole anthophyllite was derived from that of the orthorhombic pyroxene, enstatite, in the same way as that of tremolite was derived from that of diopside (*cf.* Table 1 for correspondences in cell edges and space-group symmetry).

TABLE 1. RELATIONSHIPS BETWEEN UNIT CELL AND SPACE GROUP OF MONOCLINIC AND ORTHORHOMBIC

Pyroxene		Amphibole
Diopside $C2/c$		Tremolite $C2/m$
a 9.71 Å		a 9.76 Å
b 8.89		b 17.8
c 5.24		c 5.27
β 105°		β 105.2°
	Doubling of b	
Enstatite $Pbca$	cell edge	Anthophyllite $Pnma$
a 18.2 Å	→	a 18.5 Å
b 8.87		b 17.9
c 5.20		c 5.27
Protoenstatite $Pbcn$		Protoamphibole $Pnmn$
a 9.25 Å		a 9.33 Å
b 8.74		b 17.88
c 5.32		c 5.29

The only other orthorhombic structure-type of amphibole to be described since Warren's original work is that of the synthetic amphibole, protoamphibole (Gibbs, Bloss and Shell, 1960). Because its cell edges and space group symmetry (Table 1) show the same correspondence to protoenstatite (Smith, 1959) as those of tremolite do to diopside and those of anthophyllite do to enstatite, Gibbs *et al.* (1960) were able to postulate a structure for the orthorhombic amphibole based on that of protoenstatite.

The present study was undertaken to confirm and refine the postulated structure, to establish the cation distribution Mg, Li among the M sites, to determine the distribution of the cations in the relatively large cavity (the so-called A-site) at the back of the double chain and to examine the

TABLE 2. PHYSICAL AND CHEMICAL PROPERTIES OF PROTOAMPHIBOLE

Optical properties			
λ(Å)	α	β	γ
F (4861)	1.581	1.592	1.599
D (4893)	1.575	1.587	1.593
C (6563)	1.572	1.585	1.591
$N_f - F_c$	0.009	0.007	0.008

Cell edges (Å)	Density (g cm^{-3})
a 9.330, $\hat{\sigma}$ 0.005	2.923, $\hat{\sigma}$ 0.004
b 17.879, $\hat{\sigma}$ 0.008	
c 5.288, $\hat{\sigma}$ 0.003	

Chemical analysis: (Analyst: C. O. Ingamells); SiO_2 60.6; MgO 33.4; F 5.2; Li_2O 2.3; Al_2O_3 0.3; H_2O 0.2; Na_2O 0.1; H_2O^- 0.0; H_2O^+ 0.2; Less 0=F, OH −2.2=99.9.
Unit-cell contents: $Na_{0.06}Li_{2.40}Mg_{12.88}\cdot Si_{15.68}Al_{0.08}O_{43.42}F_{4.28}OH_{0.30}$.

tetrahedral bond lengths and angles in the chain in light of Cruickshank's (1961) d-p π-bonding model.

EXPERIMENTAL

The sample selected for the study was kindly supplied by H. R. Shell of the U. S. Bureau of Mines, College Park, Maryland. The material is colorless, prismatic and possesses a perfect (110) cleavage. Its physical and chemical properties are given in Table 2. The optical properties were measured on a five-axis universal stage using a monochromatic light source and the standard single-variation technique. The density was determined by the suspension method described by Midgley (1950). The unit-cell dimensions were found from a least-squares refinement of thirty-one reflections of the powder diffraction record. C. O. Ingamells made the chemical analysis at the Mineral Constitution Laboratories at The Pennsylvania State University. The unit-cell contents were obtained by normalizing the chemical analysis in terms of the measured density and the unit-cell volume.

Weissenberg and precession photographs, exposed about the principal axes, display an orthorhombic intensity distribution of spots. The presence of hkl and $h0l$ for all orders, $hk0$ for only $h+k=2n$ and $0kl$ for $k+l=2n$, indicate the alternate space group symmetries *Pn2n* and *Pnmn*. Piezoelectric and pyroelectric tests gave no indication of a noncentrosymmetric structure, so the centrosymmetric space group *Pnmn* was provisionally adopted. Because this led to a reasonable structure that refined statisfactorily, the space group *Pnmn* is considered to be established.

In the search for a single crystal for the intensity measurement, more than fifty crystals were rejected before a suitable one was found that did not give diffuse streaks and superstructure reflections. Discussion of these diffraction effects is deferred to a later section. The crystal was a prism 0.12 mm long and 0.05 × 0.10 mm in cross-section. The intensities were recorded with the equiinclination Weissenberg camera using Robertson's (1943) multiple film technique and Ni-filtered Cu radiation and were measured by visual comparison with a specially prepared scale which had been calibrated with a photometer. About 640 intensities were recorded and these were appropriately corrected for Lorentz-polarization effects using the data reduction program PSDR of F. M. Lovell and J. H. Van den Hende (Crystal Research Laboratory, The Pennsylvania State University).

The resulting structure amplitudes were then submitted to a least-squares refinement using the positional parameters proposed by Gibbs *et al.* (1960), fully ionized atoms and a program of V. Vand and Ray Pepinsky (Crystal Research Laboratory, The Pennsylvania State University), which is based on the diagonal approximation. The refinement converged to the atomic parameters given in Table 3(I) (Gibbs, 1962) after eight cycles in which the R-factor was reduced from 37 to 15 percent. The Mg,Li distribution among the M sites established by successive difference syntheses is as follows:

$$M(1) = M(2) = M(3) \sim 1.0 \text{ Mg};$$

$$M(4) \sim 0.25 \text{ Li} + 0.75 \text{ Mg}$$

This amounts to 13 Mg cations per unit cell which is in reasonable agreement with the 12.88 Mg cations recorded in Table 2; accordingly, Mg must be restricted to the M sites. The Li cations are segregated in about 25 percent of the M(4) sites, while those remaining apparently occupy the cavity at the back of the chain. Difference maps of the cavity did not show a significant concentration of electron density which could be attributed to Li. Therefore, it was concluded that Li is randomly distributed around the periphery of the cavity rather than being rigidly fixed at its center. Because the cavity is considerably larger than the ion, it is a reasonable conclusion.

A modified version of the Busing, Martin and Levy (1962) least-squares program was used in a second refinement of the data. The refinement converged in two cycles giving the atomic parameters and the estimated standard deviations in Table 3(II) (Gibbs, 1964) and a final R-factor of 10.1 percent for all reflections, these having been weighted according to a scheme proposed by Cruickshank (1965). The atomic scattering factors used in this calculation and later ones for Mg^{2+}, Li^+ and Si^{4+} and for O^{2-} were taken from the International Tables (1962) and from Suzuki (1960), and were modified for half-ionization.

The isotropic temperature factors calculated with the Busing-Martin-Levy program are uniformly smaller than those calculated by the Vand-Pepinsky program. This discrepancy may be attributed to the fact that the Busing-Martin-Levy program is designed to apply the refined scale factor to F_{calc} whereas the Vand-Pepinsky program applies it to $|F_{obs}|$ (Geller *et al.*, 1960, 1961). The temperature factors listed in Table 3 for the two silicon atoms are lower than normal (Burnham, 1964). Actually, little significance should be attached to the absolute magnitudes of these values or to those of the other atoms because the scattering contribution from Li in the cavity at the back of the chain was not included in the least-squares calculation.

Because the intensity data used in the foregoing calculations were recorded by film methods, a second set of data was collected from the same crystal with an equiinclination Weissenberg scintillation-counter-diffractometer using Nb-filtered Mo radiation with the expectation that these data would permit a location of the fractional Li atom in the A site. As before, absorption corrections were applied to the data assuming the crystal to be cylindrical. The structural amplitudes were then submitted to a least-squares calculation using Hanson's (1965) weighting scheme, half-ionized atoms, the results of the previous refinement and the Busing *et al.* (1962) program. The refinement converged in one cycle reducing the R-factor from 0.074 to 0.053, giving the positional and thermal parameters and estimated standard deviations listed in Table 3(III). However, despite the higher precision of the counter intensity data, these results are not significantly different from those obtained with the film intensity data (Table 3(II)). Diqerence maps, calculated at ~0.1 Å intervals along z, were found to be statistically featureless, giving no indication of the cation in the cavity but confirming the Mg,Li distribution established earlier for the M sites. The more important interatomic distances and angles calculated using a program prepared by C. T. Prewitt are given in Table 4. The estimated standard deviations, given in parentheses, were calculated using the proportion of variance formula and the appro-

TABLE 3. ATOMIC PARAMETERS OF PROTOAMPHIBOLE[a]

		I	II	III
O(1)	x	0.1146	0.1144(6)[a]	0.1155(4)
	y	.0849	.0840(3)	.0851(2)
	z	.1662	.1648(9)	.1659(7)
	B	1.13	.34(9)	.56(6)
	$\langle\mu\rangle$	0.120	.066(9)	.084(4)
O(2)	x	0.1213	0.1215	0.1216(4)
	y	.1724	.1724(3)	.1726(2)
	z	.6730	.6733(9)	.6702(7)
	B	1.26	.51(9)	.64(6)
	$\langle\mu\rangle$	0.126	.080(7)	.090(4)
F	x	0.1038	0.1035(7)	0.1032(5)
	y	0	0	0
	z	.6753	.6647(10)	.6640(9)
	B	1.04	.54(11)	.70(7)
	$\langle\mu\rangle$	0.115	.083(8)	.094(5)
O(4)	x	0.1236	0.1239(6)	0.1228(4)
	y	.2506	.2508(3)	.2511(2)
	z	.1873	.1870(9)	.1844(7)
	B	1.48	.62(9)	.58(7)
	$\langle\mu\rangle$	0.137	.089(6)	.086(5)
O(5)	x	0.3479	0.3478(8)	0.3475(5)
	y	.1214	.1217(2)	.1212(3)
	z	.4276	.4299(9)	.4292(9)
	B	1.03	.43(9)	.91(8)
	$\langle\mu\rangle$	0.114	.074(8)	.107(5)
O(6)	x	0.3509	0.3508(7)	0.3506(5)
	y	.1302	.1305(3)	.1308(3)
	z	.9311	.9325(10)	.9324(9)
	B	1.34	.89(9)	1.38(8)
	$\langle\mu\rangle$	0.130	.106(5)	0.132(4)
O(7)	x	0.3518	0.3508(8)	0.3494(6)
	y	0	0	0
	z	.1600	.1601(13)	.1592(11)
	B	1.15	.65(13)	.94(9)
	$\langle\mu\rangle$	0.121	.091(9)	.109(5)
$M(1)$	x	0	0	0
	y	0.0884	0.0884(2)	0.0883(1)
	z	1/2	1/2	1/2
	B	.54	.35(7)	.53(5)
	$\langle\mu\rangle$	.083	.066(7)	.082(3)
$M(2)$	x	0	0	0
	y	0.1791	0.1793(2)	0.1786(1)
	z	0	0	0
	B	.43	.42(7)	.58(5)
	$\langle\mu\rangle$	.074	.073(6)	.086(4)
$M(3)$	x	0	0	0
	y	0	0	0
	z	0	0	0
	B	0.41	0.43(9)	0.55(6)
	$\langle\mu\rangle$	.072	.074(5)	.083(4)
$M(4)$	x	0	0	0
	y	0.2573	0.2574(2)	0.2579(1)
	z	1/2	1/2	1/2
	B	.69	.52(8)	.55(6)
	$\langle\mu\rangle$	.093	.081(6)	.083(4)
Si(1)	x	0.2866	0.2867(3)	0.2868(2)
	y	.0846	.0847(1)	.0847(1)
	z	.1702	.1704(3)	.1720(3)
	B	.53	.07(5)	.38(4)
	$\langle\mu\rangle$	.082	.028(10)	.069(4)
Si(2)	x	0.2940	0.2937(3)	0.2941(2)
	y	.1711	.1709(1)	.1711(1)
	z	.6689	.6689(3)	.6694(3)
	B	.57	.12(5)	.48(4)
	$\langle\mu\rangle$	.085	.039(8)	.078(3)

I Diagonal matrix least-squares refinement of film-recorded data. II Full matrix least-squares refinement of film-recorded data III Full matrix least-squares refinement of counter-recorded data.

[a] The estimated standard deviations are given in the parentheses following the atomic parameters: those listed for the root-mean-square displacements $\langle\mu\rangle$ were calculated using the expression $\hat{\sigma}\langle\mu\rangle=\hat{\sigma}(B)/16\pi^2\langle\mu\rangle$.

priate diagonal elements of the variance-covariance matrix. The observed and calculated structure factors are on deposit.

DISCUSSION

General description. Figures 1 and 2 are drawings of the structure of protoamphibole viewed down the c and a axes, respectively. The structure is composed of layers of interlocking $(Si_4O_{11})_\infty$ chains, the tetrahedra of which are linked together in arrays of fluorine-centered hexagonal rings. The chains are in layers parallel to (100) with their endless dimensions parallel to c (Fig. 2). Along b they alternate in orientation with the apical oxygens, O(1) and O(2), pointing successively up and down along a. The basal O(4) oxygens dovetail with the apical oxygens of adjacent chains and interlock the chains together into layers. The layers, stacked along a, are bound together by Mg,Li cations coordinated between narrow hexagonal strips composed of apical oxygen and fluorine anions, the coordination being effected by a stagger of $\sim(+c/3)$ between adjacent layers. An additional stagger of $\sim(-c/3)$ for the next layer in the sequence along a gives an overall displacement of zero between alternate layers. This accounts for

[1] To obtain a copy of structure amplitude tables, order NAPS Document #00462 from ASIS National Auxiliary Publications Service, c/o CCM Information Sciences, Inc., 22 West 34th Street, New York, New York 10001; remitting $1.00 for microfiche or $3.00 for photocopies.

TABLE 4. INTERATOMIC DISTANCES (Å) AND ANGLES (°) IN PROTOAMPHIBOLE

Si-O distances in Si(1) tetrahedron			
Si(1)-O(1)	1.592(4)	Si(1)-O(5)	1.616(5)
Si(1)-O(6)	1.623(5)	Si(1)-O(7)	1.624(2)
Mean 1.614			
O-O distances within tetrahedron about Si(1)			
O(1)-O(6)	2.642(6)	O(5)-O(6)	2.665(6)
O(1)-O(5)	2.650(6)	O(6)-O(7)	2.630(8)
O(1)-O(7)	2.654(7)	O(5)-O(7)	2.597(8)
Mean 2.640			
O-Si(1)-O bond angles			
O(7)-Si(1)-O(1)	111.2	O(7)-Si(1)-O(5)	106.6
O(5)-Si(1)-O(1)	111.4	O(6)-Si(1)-O(5)	108.8
O(6)-Si(1)-O(1)	110.5	O(6)-Si(1)-O(7)	108.2
Mean 109.45			
Si-O distances in Si(2) tetrahedron			
Si(2)-O(2)	1.605(4)	Si(2)-O(6)	1.655(5)
Si(2)-O(4)	1.592(4)	Si(2)-O(5)	1.626(5)
Mean 1.620			
O(2)-O(4)	2.742(6)	O(4)-O(6)	2.495(6)[a]
O(2)-O(6)	2.650(6)	O(4)-O(5)	2.661(6)
O(2)-O(5)	2.624(6)	O(5)-O(6)	2.634(6)
Mean 2.634			
O-Si(2)-O bond angles			
O(2)-Si(2)-O(4)	118.2	O(5)-Si(2)-O(6)	108.7
O(2)-Si(2)-O(6)	108.8	O(4)-Si(2)-O(5)	111.6
O(2)-Si(2)-O(5)	108.6	O(4)-Si(2)-O(6)	100.5[b]
Mean 109.4			
M(3)-O,F distances in *M*(3) octahedron			
M(3)-F	2.021(4)	*M*(3)-O(1)	2.062(4)
Mean 2.048			
O-O,F distances within octahedron about *M*(3)			
O(1)-F	3.061(5)	O(1)-F	2.704(5)[a]
O(1)-O(1)	3.039(10)	O(1)-O(1)	2.789(10)[b]
Mean 2.893			
O-*M*(3)-O,F angles			
O(1)-*M*(3)-O(1)	95.0°	O(1)-*M*(3)-O(1)	85.1[b]
O(1)-*M*(3)-F	97.1	O(1)-*M*(3)-F	82.9[b]
Mean 90.0			
M(1)-O,F distances in *M*(1) octahedron			
M(1)-F	2.043(4)	*M*(1)-O(2)	2.094(4)
M(1)-O(1)	2.072(4)		
Mean 2.070			
O,F-O,F distances within octahedron about *M*(1)			
2 F-O(1)	3.043(5)	2 F-O(1)	2.704(5)[a]
2 O(1)-O(2)	3.054(5)	2 O(1)-O(2)	2.851(5)[a]
2 F-O(2)	3.091(6)	1 O(2)-O(2)	2.903(10)[a]
		1 F-F	2.597(10)[a]
Mean 2.916			
O,F-*M*(1)-O,F angles			
O(1)-*M*(1)-O(2)	94.2°	O(1)-*M*(1)-O(2)	86.4[b]
F-*M*(1)-O(2)	92.9°	O(2)-*M*(1)-O(2)	87.8[b]
F-*M*(1)-O(1)	95.4°	F-*M*(1)-F	78.6[b]
		O(1)-*M*(1)-F	82.2[b]
Mean 89.0			

TABLE 4.—(*Continued*)

M(2)-O distances in *M*(2) octahedron			
M(2)-O(1)	2.179(4)	*M*(2)-O(2)	2.084(4)
M(2)-O(4)	1.989(4)		
Mean 2.084°			
O-O distances within octahedron about *M*(2)			
O(1)-O(2)	3.054(5)	O(1)-O(2)	2.851(5)[a]
O(2)-O(4)	3.059(5)	O(2)-O(4)	2.742(5)[a]
O(4)-O(4)	3.241(10)	O(1)-O(1)	2.789(10)[a]
O(1)-O(4)	2.974(5)		
Mean 2.949			
O-*M*(2)-O angles			
O(1)-*M*(2)-O(1)	91.4	O(1)-*M*(2)-O(2)	83.9[b]
O(2)-*M*(2)-O(4)	94.9	O(2)-*M*(2)-O(4)	84.7[b]
O(4)-*M*(2)-O(4)	109.2°	O(1)-*M*(2)-O(1)	79.6[b]
O(1)-*M*(2)-O(4)	90.9°		
Mean 90.0°			
M(4)-O distances in *M*(4) octahedron			
M(4)-O(2)	2.107(4)	*M*(4)-O(4)	2.029(4)
M(4)-O(6)	2.453(5)		
Mean 2.196			
O-O distances within octahedron about *M*(4)			
O(2)-O(4)	2.929(5)	O(2)-O(4)	2.742(5)[a]
O(2)-O(6)	3.740(5)	O(2)-O(2)	2.903(10)[a]
O(4)-O(6)	3.875(5)	O(4)-O(6)	2.495(5)[a]
O(6)-O(6)	2.879(10)		
Mean 3.112			
O-*M*(4)-O angles			
O(2)-*M*(4)-O(4)	90.2	O(2)-*M*(4)-O(4)	83.0°[b]
O(2)-*M*(4)-O(6)	106.0	O(2)-*M*(4)-O(2)	78.7[b]
O(4)-*M*(4)-O(6)	119.4	O(4)-*M*(4)-O(6)	66.9[b]
O(6)-*M*(4)-O(6)	71.9		
Mean 90.1			
M-*M* distances between adjacent *M*-O octahedra			
M(1)-*M*(1)	3.150(6)	*M*(1)-*M*(2)	3.099(3)
M(1)-*M*(3)	3.079(3)	*M*(1)-*M*(4)	3.035(3)
M(2)-*M*(4)	3.001(3)		
Mean 3.064			
Si-Si distances between adjacent SiO_4 tetrahedra			
Si_1-Si_2	3.052(3)	Si_1-Si_1	3.029(6)
Si_1-Si_2	3.075(3)		
Mean 3.057			
Si-O-Si angles			
Si(1)-O(1)-Si(7)	137.1°	Si(1)-O(5)-Si(2)	140.6
Si(1)-O(6)-Si(2)	140.9		
Mean 140.0			

The e.s.d. of the bond angles, calculated using an equation provided by Darlow (1960), range from 0.5 to 0.8°.

[a] Shared edge.

[b] Angle opposite shared edge.

the 9.33Å *a* cell edge (one-half that of anthophyllite) and the orthogonal geometry of the unit cell of protoamphibole. The direction of stagger can be related to the placement of the cations in the available sites of the octahedral layer. Figure 3 is a projection of the octahedral layer on (100). The cations in this layer lie above every other

triangle of the hexagonal network formed by the anions of the lower level, the upper level being staggered $\sim(+c/3)$ with respect to the lower one to effect the octahedral coordination. The direction of the layer stager is indicated in Figure 3. Note that a layer stagger of $\sim(-c/3)$ would result if the cations were shifted from their present positions to the ones above the vacant triangles of the lower level; *i.e.*, the upper level would require a stagger in the opposite direction to effect the cation coordination. The known structural types of amphibole (clinoamphibole, protoamphibole and anthophyllite) can be described in terms of ordered staggered-layer sequences of interlocking double chains. For example, the protoamphibole structure is an ordered two-layer sequence staggered $\cdots(+c/3)\ (-c/3)\cdots$ On the other hand, the anthophyllite structure with its doubled a-axis is a four-layer stacking sequence successively staggered $\cdots(+c/3)\ (+c/3)\ (-c/3)\ (-c/3)\cdots$; whereas, the clinoamphibole structure is an ordered two-layer sequence staggered $\cdots(+c/3)\ (+c/3)\cdots$ or $\cdots(Mc/3)\ (-c/3)\cdots$ (Appleman *et al.*, 1966).

A mistake in any of these ordered stacking sequences will result in the formation of a twinned crystal with (100) as the composiiton plane. However, if the number of mistakes is large, diffuse streaks will develop parallel to a^* (Wilson, 1962). It was mentioned in an earlier section that diffuse streaks and superstructure reflections were observed for many protoamphibole crystals. Figure 4 is an a-axis oscillation photograph of one such crystal, showing diffuse streaks along lines of constant zeta which connect strong reflections on adjacent layer lines. Several of the streaks are uniform in intensity whereas others have weak maxima located between the layer lines. Figure 5a is a Weissenberg photograph of the $hk1$ level showing streaks which connect spots of constant index h. Higher level photographs about c exhibit similar characteristics as do photographs obtained about b (Fig. 5b). No streaks were observed in a-axis Weissenberg photographs. The diffuse streaks parallel to a^* are evidence for randomly distributed stacking faults parallel to (100) whereas the weak maxima between the layer lines indicate that there are, in addition, ordered runs of faults with the stacking sequence $\cdots(+c/3)\ (-c/3)$ fault $(-c/3)\ (+c/3)\cdots$ Such runs correspond to the stacking sequence in anthophyllite, and account for the weak maxima located between the layer lines of the a-axis oscillation photograph (Appleman *et al.*, 1966).

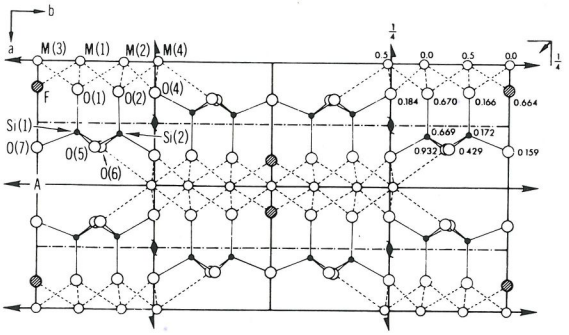

FIG. 1. The structure of protoamphibole projected down c. The large open circles represent oxygen; the diagonally hatched ones, fluorine; the small open ones, M-cations and the small solid ones, silicon. The atoms are labelled in the upper left asymmetric unit and the numbers in the upper right are the z fractional coordinates.

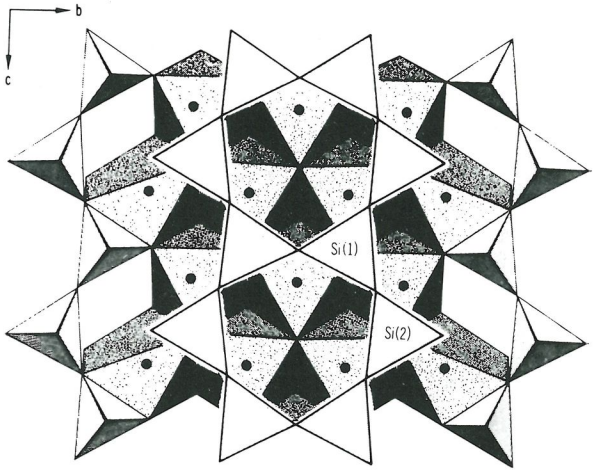

FIG. 2. The structure of protoamphibole projected down a showing the articulation of the chains to the octahedral layer.

$(Si_4O_{11})_\infty$ chains. The chains in protoamphibole (Figs. 1 and 2) consist of two nonequivalent SiO_4 tetrahedra, Si(1) and Si(2), which are rotated ($\sim$3.5°) in opposite directions about a to give the chain a slightly kinked appearance. This kinking and the slight curvature of the chains away from the plane of the octahedral cations are univer-

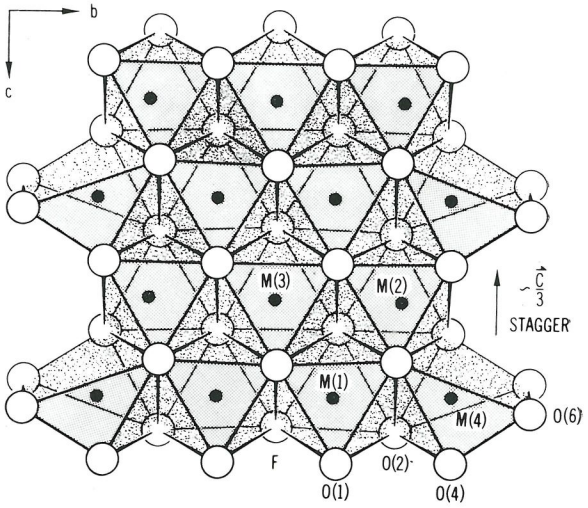

FIG. 3. The octahedral layer in protoamphibole projected down a. The vector, $\sim c/3$, defines the stagger of the upper layer of anions with respect to the lower to effect the octahedral coordination of the M cations. The large open circles represent oxygen and fluorine and the small circles, the M-cations.

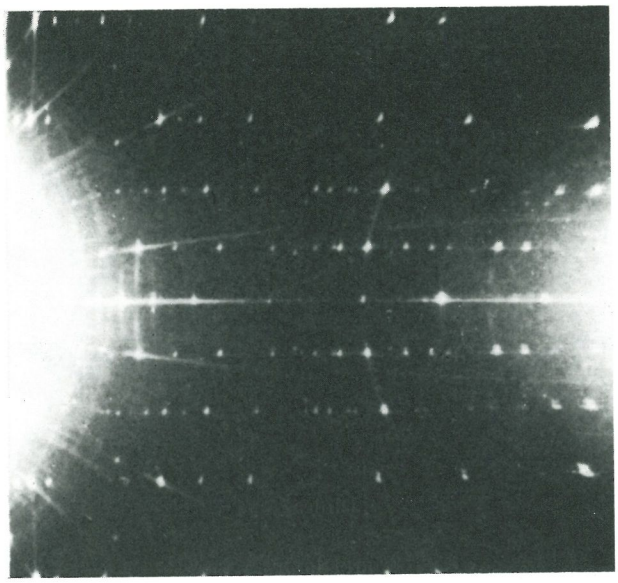

FIG. 4. A portion of an a-axis oscillation photograph of protoamphibole crystal containing stacking faults. Note the diffuse maxima (superstructure reflections) located between zero and first layer lines and the diffuse streaks connecting intense spots on adjacent layer lines.

sal among the amphiboles and have been attributed to a dimensional misfit between octahedral and tetrahedral layers (Whittaker, 1949). The tetrahedral bond-angles in the chains are consonant with such a curvature, the angles on the extended side being, on the average, 111.4°, wider than those on the compressed side, 107.4°. However, as will be considered in more detail later, these angles may in part arise from repulsion effects between adjacent Si-O bonds, particularly between those of higher π-bond order.

The range of bond-angle strains in the Si(2) tetrahedron (−9.0° to +8.7°) is about three times as great as that in the Si(1) tetrahedron (−2.9° to 1.9°). This is expected because the Si(2) tetrahedron, unlike Si(1), shares an edge, O(4)-O(6), with the $M(4)$ polyhedron. This edge, as predicted by Pauling (1929) from electrostatic considerations, is short and measures 2.495Å. Perforce the tetrahedral angle, O(4)-Si(2)-O(6) = 100.5°, opposite the shared edge is narrow and the compensating adjacent angle, O(4)-Si(2)-O(2) = 118.2°, is wide.

The Si-Si distances between first-neighbor tetrahedra in the same chain average 3.06 Å, a value slightly shorter than that (3.07 Å) recorded for both cummingtonite (Ghose, 1961; Fischer, 1966) and glaucophane (Papike and Clark, 1968).

The average Si-O bond length and the average O-Si-O and Si-O-Si bond angles are 1.617 Å, 109.4° and 140.0°, respectively. The O-Si-O angle is close to the ideal tetrahedral angle of 109.47°, and the Si-O-Si angle is identical with 140°, the mean value obtained in a statistical evaluation of bond-angles in a number of precisely refined silicates (Liebau, 1951).

The mean Si-O bond length for over fifty silicates has recently been found to increase with the average coordination of the oxygen from 1.60_8 Å for two-coordinated oxygen to 1.63_8 Å for four-coordinated oxygen (Gibbs and Brown, 1968; Shannon and Prewitt, 1969; Brown, Gibbs and Ribbe, 1969). The mean Si-O distances for the two nonequivalent tetrahedra in protoamphibole are: $\overline{\text{Si(1)-O}}$ = 1.614; $\overline{\text{Si(2)-O}}$ = 1.620 Å. The fact that the Si(2)-tetrahedron is slightly larger than Si(1) can be explained in terms of the average coordination of oxygen, *i.e.*, 2.75 for oxygens bonded to Si(1) and 3.00 for those bonded to Si(2). The Si(2)-tetrahedron in glaucophane (Papike and Clark, 1968), in cummingtonite (Ghose, 1961; Fischer, 1966) and in riebeckite (Colville and Gibbs, 1964) is also slightly larger than the Si(1)-tetrahedron, despite the differences in chemistry and in distribution and bonding characteristics of the octahedral atoms.

A preliminary refinement of an aluminous hornblende has led Papike and Clark (1967) to conclude that Al tends to segregate into the site corresponding to the smaller Si(1)-tetrahedron (designated $T(1)$ by Papike and Clark, 1967) rather than the larger Si(1) tetrahedron (designated $T(2)$ by Papike and Clark, 1967) as might be predicted from size considerations (Hume-Rothery and Powell, 1935). This conclusion suggests that charge-balance considerations are more important in dictating the distribution of tetrahedral Al and Si in hornblende than are size consider-

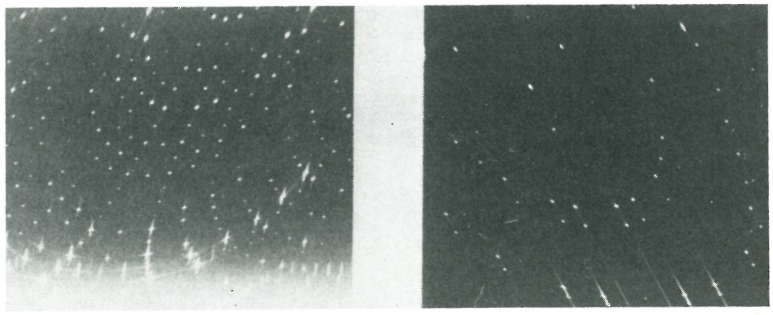

(a) (b)

FIG. 5. (a) is a portion of a c-axis Weissenberg photograph and (b) is a similar photograph recorded about b. In both, diffuse streaks lie along row-lines parallel to a^*.

ations. If this is the case, Si probably segregates into the larger Si(2)-tetrahedron because it then forms a bond with the underbonded oxygen O(4), which may result in (1) the formation of a relatively strong π-bond between Si and O(4) and a concomitant balancing of the valency of O(4) in accord with the electroneutrality principle (Pauling, 1948; Waser, 1968) and (2) an explanation for the Si(2)-O(4) bonds which are characteristically shortest in cummingtonite (1.613 Å; Fischer, 1966), riebeckite (1.606 Å; Colville and Gibbs, 1964), glaucophane (1.594 Å; Papike and Clark, 1968) and protoamphibole (1.592 Å). However, should Al segregate at the larger site, the valency of O(4) would likely remain unsatisfied because of the lesser charge of Al^{3+} and the lesser ability of Al to form a π-bond with oxygen (Brown *et al.*, 1969). In many amphiboles, Al replaces Si in the $(Si_4O_{11})_\infty$ chain up to the extent $(Si_3AlO_{11})_\infty$; this limiting composition is explained if Al segregates only into the Si(1) site and if the aluminum avoidance rule is observed (Loewenstein, 1954; Goldsmith and Laves, 1955).

Two types of Si-O bonds can be distinguished in the chain of protoamphibole: (1) those to the nonbridging oxygens, O(nbr), bonded to one Si and to two or three *M* cations [Si(1)-O(1) = 1.592; Si(2)-O(4) = 1.592; Si(2)-O(2) = 1.605 Å] and (2) those to the bridging oxygens, O(br), bonded to two silicon atoms and to zero or one *M* cation [Si(1)-O(5) = 1.616; Si(1)-O(6) = 1.623; Si(1)-O(7) = 1.624; Si(2)-O(5) = 1.626; Si(2)-O(6) = 1.655 Å; Gibbs, 1964 and Table 5, this paper]. Each of these bond lengths is consistent with Cruickshank's model for *d-p* π-bond formation in silicates, *i.e.*, the Si-O bonds to nonbridging oxygens (higher π-bond order) are shorter than those to the bridging oxygens (lower π-bond order). However, this does not hold true for all the Si-O bonds of a number of other amphiboles (Ghose, 1961; Colville and Gibbs, 1964; Papike and Clark, 1968) where, in addition to Mg^{2+}, the nonbridging oxygens are bonded to cations of greater electronegativity (Al^{3+}, Fe^{3+}, Fe^{2+}) and where some of the Si-O(nbr) bonds are as long or longer than the Si-O(br) bonds. These variant bonds lengths are possibly due to the formation of partially covalent bonds between O(nbr) and the cations Fe^{3+}, Al^{3+}, and Fe^{2+}. Such covalent bonds would drain some of the π-electrons from the Si-O(nbr) system to weaken and lengthen the bond between Si and O(nbr). Cruickshank (1961) has proposed a similar mechanism to explain the Si-O bond lengths in thortveitite.

Papike and Clark (1968) have indicated that "any observed lengthening of the *T*(2)-O(2) and *T*(2)-O(4) bonds should be a significant indicator of Al or Fe substitution in the T(2) site." However, this generalization is not supported by the Si-O distance in protoamphibole and cummingtonite which contain *only* Si in tetrahedral coordination. In protoamphibole Si(2)-O(2) = 1.605 and Si(2)-O(4) = 1.592 Å, whereas in cummingtonite (Fischer, 1966) Si(2)-O(2) = 1.625 and Si(2)-O(4) = 1.612 Å. These bond lengths differ by 0.02 Å; thus it is apparent that before the "lengthening" of these bonds can be employed to predict Al/Fe substitution, the effects of neighboring *M*-cations need to be assessed as well.

If the Si-O bonds to the nonbridging oxygens in protoamphibole are of higher π-bond order than those to bridging oxygens, and if the nonbonding electron pairs of oxygen can be practically neglected, then the angles in the tetrahedra of the chain should decrease in the order O(nbr)-Si-O(nbr) > O(br)-Si-O(nbr) > O(br)-Si-O(br) (Gillespie, 1963). In all cases for the Si(1) tetrahedron, the O(br)-Si-O(nbr) angles [O(6)-Si(1)-O(1) = 110.5; O(5)-Si(1)-O(1) = 111.4°; O(7)-Si(1)-O(1) = 111.2°] are two to five degrees wider than the O(br)-Si-O(br) angles [O(5)-Si(1)-O(6) = 108.8°; O(5)-Si(1)-O(7) = 106.6°; O(7)-Si(1)-O(6) = 108.2]. This is expected because in theory the higher π-bond-order Si-O(nbr) bonds should repel the lower π-bond-order Si-O(br) bonds more than the latter repel one another. As indicated earlier, these angles are also expected if the curvature of the chain result from a dimensional misfit between tetrahedral and octahedral layers. However, both mechanisms should not be regarded as mutually exclusive but rather as complementary; they simultaneously minimize (1) the strain energy inherent in the dimensional misfit and (2) the repulsive forces between adjacent Si-O bonds to bridging and nonbridging oxygens.

The angles in the Si(2)-tetrahedron are further complicated by a shared edge which is short and which necessitates a narrow O(6)-Si(2)-O(4) angle of 100.5°. Since this angle is of the type O(br)-Si-O(nbr), there must be an increase in the potential energy of the system if repulsive forces are operative between the two bonds comprising the angle as well as between the two oxygens comprising the edge (McDonald and Cruickshank, 1967). However, this increase is very likely more than compensated by the decrease in potential energy attending the increased cation-cation distance and the more effective shielding of the shared-edge configuration.

The only angle in the chain of the type O(nbr)-Si-O(nbr) exists in the Si(2)-tetrahedron, O(2)-Si(2)-O(4) = 118.2°. As expected it is the widest tetrahedral angle, but it is difficult to decide unequivocally whether the angle is adopted primarily because of geometrical factors (compensating the narrow O(6)-Si(2)-O(4) angle) or because of electrostatic factors (repulsion between Si-O bonds) or both. However, if the π-bond order of the Si-O(nbr) bonds is greater than that of the Si-O(br) bonds then the angle probably is dictated by the best energetic compromise between both factors. Of the remaining angles in the tetrahedron, O(5)-Si(2)-O(6) = 108.7° and O(5)-Si(2)-O(4) = 111.6° are consistent with the theory whereas O(5)-Si(2)-O(2) = 108.6 and O(6)-Si(2)-O(2) = 108.8° are not, the latter being of the same magnitude as those of the type O(br)-Si-O(br). However, examination of the geometry of the tetrahedron shows that these angles must be the same size as O(5)-Si(2)-O(6) under the constraints imposed by

the narrow angle opposite the shared-edge and the wide one between the two Si-O(nbr) bonds. Wider O(5)-Si(2)-O(2) and O(6)-Si(2)-O(2) angles would require that the angle opposite the shared-edge be wider and that between the two Si-O(nbr) bonds be narrower, a feature which apparently cannot develop without disrupting the compromise adopted between competing geometrical and bonding factors. Although a crystal structure will not form unless most of the geometrical and bonding requirements are satisfied, it is doubtful if all the requirements will be satisfied exactly in a complex structure like protoamphibole. Nevertheless, on the basis of the evidence provided by protoamphibole as well as by haradaite (Takéuchi and Joswig, 1967), pectolite (Prewitt, 1967), α-$Na_2Si_2O_5$ (Pant and Cruickshank, 1968), datolite (Pant and Cruickshank, 1967), β-$Na_2Si_2O_5$ (Pant, 1968) and the framework silicates (Brown *et al.*, 1969), it appears that Cruickshank's *d-p* π-bonding model provides a working hypothesis within which many of individual bond lengths and angles in silicates can be qualitatively understood, despite the complicating geometrical and electrostatic factors introduced by shared edges, bond-angle strains and effects of nontetrahedral cations.

Octahedral layer. The octahedral layer in protoamphibole is viewed down *a* in Figure 3. The cations in the layers are repelled from one another a significant but small amount with those in the polyhedron about $M(2)$ being displaced toward the periphery of the layer. In this process, the shared edges become shorter, thereby partially shielding the coordinated cations. Accordingly, the shared edges range in length from 2.50 to 2.90 Å in contrast to the unshared edges (2.85 to 3.7 Å). In addition, the O-M-O angles to the unshared edges are wider, on the average, than those to the shared edges. As the shared edges of the octahedral layer are shorter than the unshared ones, the layer is slightly flattened, a feature also observed in pyroxene and mica.

The octahedra about $M(1)$ and $M(3)$ are nearly regular with mean bond lengths $\overline{M\text{-O,F}}$ 2.070 and 2.048 Å, respectively, while that about $M(2)$ is slightly more irregular with bond lengths ranging from 1.989 to 2.179 Å, the average M-O being 2.084. The six-coordinated $M(4)$ polyhedron is very irregular and closely resembles $M(1)$ in protoenstatite (Smith, 1959) because there are blocks of that structure incorporated in protoamphibole. Two of the bonds, $M(4)$-O(2) and $M(4)$-O(4), respectively, measure 2.107 and 2.029 Å, whereas a third, $M(4)$-O(6) = 2.453 Å is about 0.4 Å longer. Inasmuch as the $M(4)$-O(5) = 3.442 Å distance is relatively long, the O(5) atom is not considered part of the $M(4)$ coordination polyhedron. This polyhedron, as mentioned earlier, has a short edge, O(4)-O(6) = 2.495 Å, which is shared with the Si(2) tetrahedron.

The cation distribution among the M-sites determined by structure analysis of a number of amphiboles (Appleman *et al.*, 1966) indicate that the larger M-cations tend to concentrate at the larger $M(4)$ site whereas the smaller ones concentrate in the smaller $M(1)$, $M(2)$ and $M(3)$ sites. In protoamphibole, the concentration of the larger Li(r = 0.74 Å) in about 25 percent of the $M(4)$ sites with Mg(r = 0.70 Å) filling the rest as well as the smaller M-sites is consonant with this conclusion. Gibbs and Prewitt (1966) have found that when cations of appreciably different radii randomly occupy an M-site, that their isotropic temperature factors (B), as well as those of the coordinating anions, are larger than those recorded for sites containing cations of similar radii. The B's calculated for Mg,Li at $M(4)$ are statistically identical with those calculated for Mg at $M(1)$, $M(2)$ and $M(3)$ (Table 5) confirming that the radii of Mg and Li are similar (Shannon and Prewitt, 1969). The B's of O(2) and O(4) coordinating Mg,Li are nearly identical with those of the anions coordinating Mg. The B of the remaining anion O(6) coordinating Mg,Li is more than twice as large as those of O(2) and O(4). However, this larger B along with those calculated for O(5) and O(7) probably reflects their lower coordination numbers (Burnham, 1964) rather than cation disorder.

Finally, as indicated earlier, difference maps failed to show a significant concentration of electron density in the A-site attributable to Li. Nevertheless, the short O(5)-O(7) edge of the Si(1) tetrahedron suggests that the Li is bonded to both these anions thereby forming a short edge shared in common with Si(1) and Li. However, an attempt to locate Li from geometrical considerations with respect to O(5) and O(7) and refine the position by least-squares methods failed.

Acknowledgments

It is a pleasure to thank Professors F. D. Bloss and P. H. Ribbe of Virginia Polytechnic Institute at Blacksburg, Virginia for their critical reviews of the final manuscript. H. R. Shell of the U. S. Bureau of Mines at College Park, Maryland donated the sample for the structure analysis and C. O. Ingamells of the U. S. Geological Survey at Menlo Park, California made the chemical analysis.

References

Appleman, D. E., F. R. Boyd, Jr., G. M. Brown, W. G. Ernst, G. V. Gibbs and J. V. Smith (1966) *Chain Silicates*. Amer. Geol. Inst., Washington, D.C.

Brown, G. E., G. V. Gibbs, and P. H. Ribbe (1969) The nature and the variation in length of the Si-O and Al-O bonds in framework silicates (abstr.) *Trans. Amer. Geophy. Union* **50**, 358.

Burnham, C. W. (1964) Temperature parameters of silicate crystal structures (abstr.) *Mineral Soc. Amer. Summer Meet., Bozeman, Montana*, 7.

Busing, W. R., K. O. Martin, and H. A. Levy (1962) ORFLS, A fortran crystallographic least-squares program. *U.S. Clearinghouse Fed. Sci. Tech. Info. Doc.* **ORNL-TM-305.**

Colville, A., and G. V. Gibbs (1964) Refinement of the crystal

structure of riebeckite (abstr.). *Geol. Soc. Amer. Meet.* [*Geol. Soc. Amer. Spec. Pap.* **82,** 31 (1965)].

CRUICKSHANK, D. W. J. (1961) The role of 3*d*-orbitals in π-bonds between (a) silicon, phosphorus, sulphur, or chlorine and (b) oxygen or nitrogen, *J. Chem. Soc.,* **1961,** 5486–5504.

——— (1965) Errors in least-squares methods, *In,* J. S. Rollett, Ed., *Computing Methods in Crystallography,* Pergamon Press, New York, N.Y.

DARLOW, S. F. (1960) Errors in bond angles. *Acta Crystallogr.* **13,** 683.

FISCHER, K. F. (1966) A further refinement of the crystal structure of cummingtonite, $(Mg,Fe)_7(Si_4O_{11})_2(OH)_2$ *Amer. Mineral.* **51,** 814–818.

GELLER, S., AND J. L. DURAND (1960) Refinement of the structure of $LiMnPO_4$. *Acta Crystallogr.* **13,** 325–331.

——— AND ——— (1961) Parameter interaction in least-squares refinement. *Acta Crystallogr.* **14,** 1026–1035.

GHOSE, S. (1961) The crystal structure of a cummingtonite. *Acta Crystallogr.* **14,** 622–627.

GIBBS, G. V. (1962) *The Crystal Structure of Protoamphibole.* Ph.D. Thesis, The Pennsylvania State University.

——— (1964) Crystal structure of protoamphibole (abstr.). *Geol. Soc. Amer. Ann. Meet.* [*Geol. Soc. Amer. Spec. Pap.* **82,** 71 (1965)].

———, F. D. BLOSS, AND H. R. SHELL (1960) Protoamphibole, a new polytype. *Amer. Mineral.* **45,** 974–989.

———, AND G. E. BROWN (1968) Oxygen coordination and the Si-O bond [abstr.]. *Geol. Soc. Amer. Southeastern Sec. Meet., Durham, N.C.,* 89.

———, AND C. T. PREWITT (1966) Amphibole cation site disorder (abstr.). *Int. Mineral. Ass. 5th Meet., Cambridge, England* [*In International Mineralogical Association, Papers and Proceedings of the Fifth General Meeting.* Mineralogical Society, London, p. 334–335 (1968)].

GILLESPIE, R J. (1963) The valence-shell electron-pair repulsion (VSEPR) theory of directed valency. *J. Chem. Ed.* **40,** 295–301.

GOLDSMITH, J. R., AND F. LAVES (1955) Cation order in anorthite ($CaAl_2Si_2O_8$) as revealed by gallium and germanium substitutions. *Z. Kristallogr.* **106,** 213–226.

HANSON, A. W. (1965) The crystal structure of the azulene, S-trinitrobenzene complex. *Acta Crystallogr.* **19,** 19–26.

HUME-ROTHERY, W., AND H. M. POWELL (1935) On the theory of super-lattice structures in alloys. *Z. Kristallogr.* **91,** 23–47.

LIEBAU, F. (1961) Untersuchungen über die Grosse des Si-O-Si Valenzwinkels. *Acta Crystallogr.* **14,** 1103–1109.

LOEWENSTEIN, W. (1954) The distribution of aluminum in the tetrahedra of silicates and aluminates. *Amer. Mineral.* **39,** 92–96.

MCDONALD, W. S., AND D. W. J. CRUICKSHANK (1967) A reinvestigation of the structure of sodium metasilicate, Na_2SiO_3. *Acta Crystallogr.* **22,** 37–43.

MIDGLEY, M. G. (1951) A quick method of determining the density of liquid mixtures. *Acta. Crystallogr.* **4,** 565.

PANT, A. K. (1968) A reconsideration of the crystal structure of β-$Na_2Si_2O_5$. *Acta Crystallogr.* **B24,** 1077–1083.

———, AND D. W. J. CRUICKSHANK (1967) A reconsideration of the structure of datolite, $CaBSiO_4(OH)$. *Z. Kristallogr.* **125,** 286–295.

———, AND ——— (1969) The crystal structure of α-$Na_2Si_2O_5$. *Acta Crystallogr.* **B24,** 13–19.

PAPIKE, J. J., AND J. R. CLARK (1967) The crystal-chemical role of potassium and aluminum in a hornblende of proposed mantle origin (abstr.). *Geol. Soc. Amer. Ann. Meet.* [*Geol. Soc. Amer. Spec. Pap.* **115,** 171 (1968)].

———, AND ——— (1968) The crystal structure and cation distribution of glaucophane. *Amer. Mineral.* **53,** 1156–1173.

PAULING, L. (1929) The principles determining the structure of complex ionic crystals. *J. Amer. Chem. Soc.* **51,** 1010–1026.

——— (1948) The modern theory of valency. *J. Chem. Soc.,* 1461–1467.

PREWITT, C. T. (1967) Refinement of the structure of pectolite, $Ca_2NaHSi_3O_9$. *Z. Kristallogr.* **125,** 298–315.

ROBERTSON, J. M. (1943) Technique of intensity measurements in x-ray crystal analysis by photographic methods. *J. Sci. Instr.* **20,** 175–179.

SHANNON, R. D., AND C. T. PREWITT (1969) Effective ionic radii in oxides and fluorides. *Acta Crystallogr.* (in press).

SMITH, J. V. (1959) The crystal structure of protoenstatite, $MgSiO_3$. *Acta Crystallogr.* **12,** 515–519.

———, AND S. W. BAILEY (1963) Second review of Al-O and Si-O tetrahedral distances. *Acta Crystallogr.* **16,** 801–811.

SUZUKI, T. (1960) Atomic scattering factor for O^{2-}. *Acta Crystallogr.* **13,** 279.

TAKÉUCHI, Y., AND W. JOSWIG (1967) The structure of haradaite and a note on the Si-O bond lengths in silicates. *Mineral. J.* [*Tokyo*] **5,** 98–123.

WARREN, B. E. AND W. L. BRAGG (1928) The structure of diopside, $CaMg(SiO_3)_2$. *Z. Kristallogr.* **69,** 168–193.

——— (1929) The structure of tremolite, $H_2Ca_2Mg_5(SiO_3)_8$. *Z. Kristallogr.* **72,** 42–57.

———, AND D. I. MODELL (1930) The structure of anthophyllite $H_2Mg_7(SiO_3)_8$. *Z. Kristallogr.* **75,** 161–178.

WASER, JÜRG (1968) Pauling's electroneutrality principle and the beginner, *In,* A. Rich and W. Davidson, eds., *Structural Chemistry and Molecular Biology.* W. H. Freeman and Co., San Francisco.

WHITTAKER, E. J. W. (1949) The structure of Bolivian crocidolite. *Acta Crystallogr.* **2,** 312–317.

WILSON, A. J. C. (1962) *X-ray Optics.* John Wiley and Sons, Inc., New York, N.Y.